BIOLOGY LETTERS

royalsocietypublishing.org/journal/rsbl

Research

Cite this article: O'Connor J, Marugán-Lobón J. 2026 Evaluating variation in Solnhofen avialans. *Biol. Lett.* **22**: 20250601.
https://doi.org/10.1098/rsbl.2025.0601

Received: 25 September 2025
Accepted: 14 January 2026

Subject Category:
Palaeontology

Subject Areas:
palaeontology, taxonomy and systematics, evolution

Keywords:
morphometrics, Urvogel, *Archaeopteryx*, *Anchiornis*, Avialae, growth

Author for correspondence:
Jingmai O'Connor
e-mail: joconnor@fieldmuseum.org

Electronic supplementary material is available online at https://doi.org/10.6084/m9.figshare.c.8342754.

THE ROYAL SOCIETY PUBLISHING

Evaluating variation in Solnhofen avialans

Jingmai O'Connor[1] and Jesús Marugán-Lobón[2]

[1]Field Museum of Natural History, Chicago, IL, USA
[2]Universidad Autonoma de Madrid, Madrid, Spain

JO, 0000-0002-3898-8283

As the oldest known fossil bird, *Archaeopteryx* is pivotal to the study of avian origins. Fifteen avialan fossils have been described from the Upper Jurassic Solnhofen Limestones, 14 of which have been referred to *Archaeopteryx*. Recently, this sample has been hypothesized to include archaeopterygids, non-archaeopterygid avians and anchiornithines, although interpretations concerning newly erected non-archaeopterygid avialans have not been critically examined, and currently, there is no taxonomic consensus. Morphometrics, as a powerful tool for understanding variation within a sample, can recognize non-random patterns that can support taxonomic hypotheses. Here, we analyse linear skeletal measurements from all Solnhofen avialans and compare them to the non-avian avialan *Anchiornis*. Results strongly suggest all Solnhofen avialans belong to a single taxon conforming to a growth curve. If more than one taxon is represented within the sample, these taxa are proportionately indistinguishable when growth is considered. Results also indicate that, while the forelimb becomes proportionately longer with increasing maturity, the opposite pattern is observed in *Anchiornis*, supporting interpretations that anchiornithines are non-volant. We examine the validity of the genera *Ostromia* and *Alcmonavis* and argue that purported diagnostic features do not provide robust support for their distinctiveness. Our results suggest that all known Solnhofen avialans represent *Archaeopteryx*.

1. Introduction

Archaeopteryx is arguably one of the most important and highly studied fossil taxa [1]. First described in 1861, *Archaeopteryx* remains the oldest and most basal known fossil bird [2]. Although the recent discovery of slightly younger Jurassic bird fossils with derived morphologies of the pectoral girdle suggests avian flight originated well before 150 Ma [3], until the discovery of such older fossils, *Archaeopteryx* will remain central to investigations seeking to elucidate the origin of Aves and dinosaur flight [4]. The importance of *Archaeopteryx* is influenced by the fact it is represented by several nearly complete specimens preserving soft tissues of the wing that provide ample evidence through which to explore the transition from terrestrial non-avian dinosaur to volant bird [1,4–6].

Archaeopteryx, also referred to as the 'Urvogel' (meaning 'primeval bird' in German), comes from approximately 150 Ma Upper Jurassic limestones exposed in southern Germany, collectively referred to as the Solnhofen Limestones or Plattenkalk [1,7]. Fifteen skeletal avialan specimens have been described from these deposits [1,4–10]. One was described as a non-archaeopterygid avian, *Alcmonavis poeschli* (hereafter *Alcmonavis*) [8], and 14 are generally considered to represent *Archaeopteryx* and referred to numerically, based on the sequence in which they were described, and by the city in which they permanently reside (table 1). However, the taxonomy of *Archaeopteryx* is far from resolved.

Table 1. Published measurements of all 15 Solnhofen avialans in mm. Measurements from right and left elements, when available, were averaged. As a consequence of poor preservation, the published measurements for the Haarlem specimen are estimates.

specimen		skull length	scapula	humerus	ulna	radius	meta-carpal I	meta-carpal II	meta-carpal III	ilium	femur	tibia	meta-tarsal III	taxonomy	reference
London	1st	62.5		74.6	67.2	64.7		34.4			61	80.7	44.1	*Archaeopteryx*	[1]
Berlin	2nd	52		63.5	55	54.4	8.3	28	24.8		52.6	68.5	37	*Archaeopteryx*	[1]
Maxberg (lost)	3rd			71.2	62						56.4	76.5		*Archaeopteryx*	[1]
Haarlem	4th						10.5		23.2			80	48	*Ostromia*	[1]
Eichstätt	5th	39		41.5	36.5	35	5.5	17.8	16.5		37	52.5	30.2	*Archaeopteryx*	[1]
Solnhofen	6th	65		83	72	69					67	92	47.5	*Archaeopteryx*	[1]
Munich	7th	45		57.5	53.5	53.2	7.2	24.5	23.5		48	73	40	*Archaeopteryx*	[1]
Daiting (EMK002)	8th			55.5										*Archaeopteryx*	[1]
Bürgermeister-Müller	9th			70.1	62	59	10	31.3	27.5					*Archaeopteryx*	[1]
Thermopolis	10th	52.9		56.9	50.9		6.6	23.5	22		50.3	74.6	39.6	*Archaeopteryx*	[1]
11th	11th		44.4	65.5	62.5	62	9.9	31.5	31.5	37.1	55.3	76.3	40.85	*Archaeopteryx*	[5]
12th	12th	56	43	61	55	54.4	6.6	28.2	27.2		53	66	34	*Archaeopteryx*	[9]
Karlsruhe	13th			57.8	52.8	51.3								*Archaeopteryx*	[7]
Chicago	14th	40.56	22.55	40.65	36.44	35.57	5.54	19	17.5	10.96	36.14	52.5	29.39	*Archaeopteryx*	[4]
SNSB-BSPG 2017 I 133				90	82			40.9	36.8					*Alcmonavis*	[8]

The "Daiting" specimen is now part of the permanent collection of the Evolution Museum Knuthenborg in Bandholm, Denmark.

Nearly every known specimen has been assigned a unique taxonomic identity at some point in its history [1]. In a recent study including a revised diagnosis for the genus, all well-preserved specimens were considered referrable to *Archaeopteryx* [9]. Understandably, morphology is less clear in incomplete and poorly preserved specimens, leading to taxonomic uncertainties. The Haarlem *Archaeopteryx* [11], a fragmentary and poorly preserved specimen originally identified as a pterosaur [12], has been recently reinterpreted as an anchiornithine, a clade commonly resolved as the sister clade to birds, and given the name *Ostromia crassipes* (hereafter *Ostromia*) [10]. Similarly, the specimen used to erect *Alcmonavis* is incomplete and poorly preserved, crushed in two dimensions [8]. A total of four *Archaeopteryx* species are variably considered valid [13–15]; however, with even generic identifications uncertain, we do not examine specific-level taxonomy here. The lack of consensus regarding *Archaeopteryx* taxonomy prevents known specimens from being used as a single sample to explore aspects of biology, like growth and intraspecific variation.

Several previous morphometric analyses have concluded that sampled specimens form an allometric growth curve [16,17]. The recent discovery of significant new material (six new specimens since 2005) warrants re-examination of all known specimens of Solnhofen avialans. Some previous analyses incorporated unreliable measurements, such as tail length (the tail is incomplete in most specimens) [4,9,16], or omitted specimens based on morphology-based taxonomic hypotheses [16]. Although morphometrics was used as an argument in favour of the reinterpretation of the Haarlem specimen as an anchiornithine, only six specimens were analysed [10]. Here, we conduct the first morphometric analysis of all known Solnhofen avialans and examine the validity of *Ostromia* and *Alcmonavis*. We show that both morphometric data and preserved morphology support interpretation of all specimens as a single taxon.

2. A note on taxonomy

Prior to the discovery of the Anchiornithinae, Gauthier proposed that the node referred to previously as Aves or the '*Archaeopteryx* node' (the clade formed by the common ancestor of *Archaeopteryx* and *Passer* and all its descendants, here considered to represent all birds) be renamed Avialae with Aves used for crown birds [18]. Currently, crown birds are more often referred to as Neornithes, and Aves is either still used for the '*Archaeopteryx* node', e.g. [4], or abandoned entirely [19]. Anchiornithinae is commonly recovered as more closely related to birds than to *Dromaeosaurus* and *Troodon* and thus also considered avialans [20]. However, Anchiornithinae is the sister taxon to the '*Archaeopteryx* node', which has typically not been labelled [3,21]. We propose that the '*Archaeopteryx* node' return to Aves, following [22], with the clade formed by Anchiornithinae and this node remaining Avialae such that anchiornithines are non-avian avialans. However, it is worth noting that the phylogenetic relationships of these taxa are not certain, and some cladistic analyses resolve anchiornithines as troodontids and part of Deinonychosauria [23], so all taxa discussed here (and collectively referred to as avialans) may alternatively represent paravians (all taxa more closely related to Neornithes than *Oviraptor*, *sensu* [24])—the clade that encompasses Avialae and Troodontidae.

3. Methods

Length measurements were obtained for all 15 Solnhofen avialans from the literature [1,4,5,7–9] (table 1). Twelve measurements were selected based on preservational limitations to maximize available data. Measurements for *Anchiornis* were also taken from the literature [25–27] (table 2). Only three specimens preserved all measured elements. Moreover, error accumulates in smaller bones, making it safer to operate with long bones (i.e. minimize error). To mitigate the impact of missing data on the statistical analyses and degrees of freedom resulting from random preservation, we applied an estimation based on a stochastic regression imputation (SRI) [28]. This estimates missing data by modelling correlations across the full set of variables (i.e. linear scaling), thereby preserving the original structure of the dataset, as is likely preferable over others (e.g. iterative imputation) [29]. Moreover, SRI is particularly appropriate for samples spanning a wide size range but constrained by a highly consistent scaling pattern, as in *Confuciusornis* [30], a condition also met by *Archaeopteryx* and *Anchiornis* (verified from literature and the data).

We implemented SRI in SPSS [31], imputing values for only cranial and long-bone measurements (femur, tibiotarsus, humerus, ulna and radius), while accounting for their distinct scaling patterns. The long bones of *Archaeopteryx* and *Anchiornis* scale in a largely isometric fashion (tested with the data), meaning that variation in any one element can reliably predict the others. The skull scales slightly different, but it was left for consistency of encompassing cranial and postcranial data. Five iterations of imputations were carried out, and the resulting datasets were averaged to produce a single dataset for the general analyses. We used multiple imputations based on strong ontogenetic allometries within each taxon, which provided highly accurate predictions for missing values. The imputation models were applied to the combined sample (i.e., without taxon-specific weighting) and implemented in both directions (i.e., predictor-to-predicted and predicted-to-predictor directions) to account for the asymmetry of regression models. For three incomplete specimens, most values were model-driven. To avoid over-interpreting these, we excluded and repeated all analyses. Results were qualitatively identical, indicating that the inferred patterns do not depend on these highly imputed cases. Unlike imputations based on single-variable estimates or weakly constrained models, our imputations are restricted by tight ontogenetic scaling relationships in both taxa, which limit the range of plausible values, making the procedure biologically robust.

We report graphically the variance–covariance matrix of the original dataset and the SRI imputation to show the scaling pattern between measurements and contrast with the estimated values (figure 1). Principal component (PC) analyses (PCAs) were then conducted only on the SRI datasets to summarize scaling patterns, with loadings representing the projection of measurements on the PCA eigenvectors (figure 2, table 3).

Table 2. Published measurements of *Anchiornis* in mm. BNHMC, Beijing Natural History Museum; LPM, Liaoning Provincial Museum; IVPP, Institute of Vertebrate Paleontology and Paleoanthropology; PKUP, Peking University Paleontology Department.

specimen	skull length	scapula	humerus	ulna	radius	meta-carpal I	meta-carpal II	meta-carpal III	ilium	femur	tibia	meta-tarsal III	reference
LPM-B00169	63.7	45.2	69	55.1	54	12.4	33.9	30.5	37.4	66.2	106.4	55.2	[21]
IVPP V14378		26.8	41.5	37.1					26.2	43.2	67.8		[20]
PKUP 1068			72.2	58.75	52.4	12.55	33.565	29.8	45.15	89.25	114.85	53.95	[22]
BMNHC PH804	43.5	29.1	45.7	39.8	39.1				25.1	50.9	69.5		[22]
BMNHC PH822	61.2	40.8	61.8	58.9	58.9	12.6	36.2	32.7	34.8	70.5	108.6	58	[22]
BMNHC PH823	56	40.1	65.2						40.9	68.7	95.2	51.2	[22]

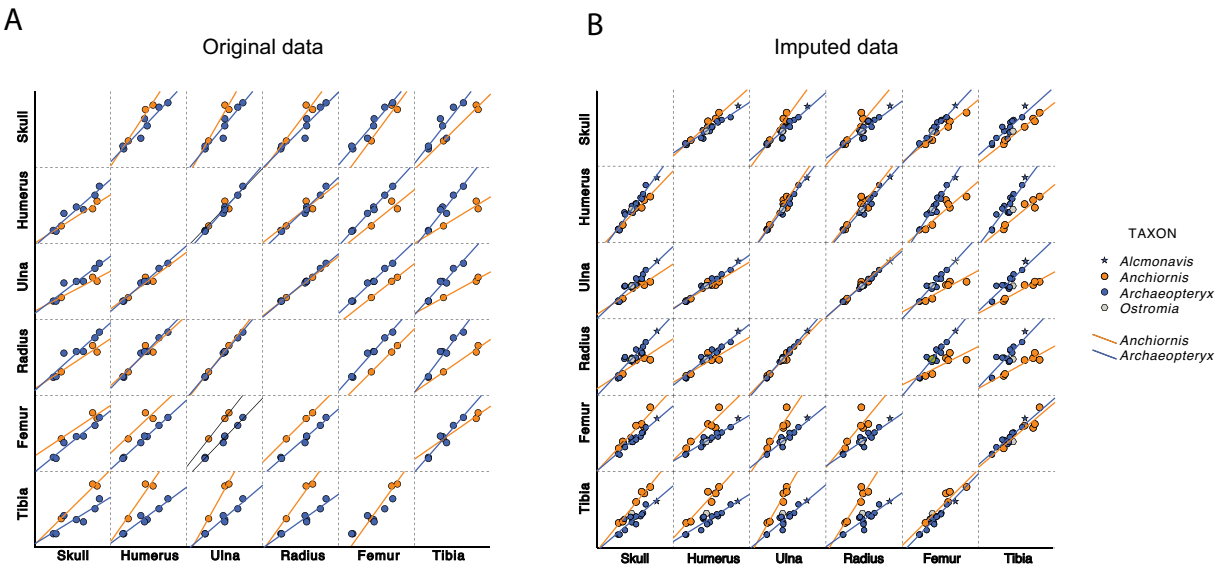

Figure 1. Scatterplots showing pairwise comparisons between the original measurements of long bones (left) and the combined set of original plus estimated values (right) for Solnhofen avialans and *Anchiornis*. Scores are omitted to allow the figures to convey the underlying trends more directly—namely, the linear isometric size scaling (small to large) and the differing slopes that denote allometric contrasts between forelimb and hindlimb bones. Smaller blue dots (right) distinguish original from imputed values. Note how the inference produces a different fit—yet expected, given its scaling relationship with the humerus—between the femur (hindlimb) and the ulna and radius (forelimb), once imputed values are included.

4. Results

(a) Morphometric analysis

The long-bone measurements scale isometrically, as shown in the dispersions of the variance–covariance matrix and their loadings on PCs (table 3; figure 1). Solnhofen avialans show a tighter fit than *Anchiornis* specimens, exemplified by the femur and humerus (i.e. between bones belonging to hindlimb and forelimb, respectively). Noticeably, the scaling slopes clearly differ between *Archaeopteryx* and *Anchiornis*, including the scaling of the skull and between limbs, indicating different growth rates.

The congruence of global scaling relationships and distributions across original data and the imputations indicates that the estimated values approximate a simulation of the expected variation, substantiating utilizing only the imputed values on the PCA. Moreover, this congruence coherently mitigates the effect of missing measurements in the expected scaling relationships between forelimb and hindlimb bones (e.g. ulna versus femur). The first two PCs together accounted for 96.1% of the total variance in the dataset, with PC1 explaining 81% and PC2 15.1%, making PC3 largely negligible, and their loadings yield a congruent pattern with the dispersions of the pairwise comparison (figure 2; table 3). PC1 exhibits almost uniformly high positive loadings across all measured variables and is unambiguously interpreted as a general size axis. PC2 captures the major axis of shape variation (limb proportions), contrasting the forelimb and hindlimb elements: it has positive loadings for forelimb bones and negative loadings for hindlimb bones, reflecting opposing allometric trends. This indicates that PC2 encapsulates the differential scaling relationships between thoracic and pelvic limb elements.

The PC1–PC2 scatter plot reveals a clear separation between Solnhofen avialans and *Anchiornis*, with no overlap in the ordination space (figure 2). This reflects the proportionately longer hindlimbs of *Anchiornis*. The direction towards positive values along PC1 corresponds to larger individuals of both taxa—i.e. growth—and the divergence along PC2 in both taxa, becoming most pronounced around intermediate PC1 values (at mid-size stages), suggests that divergence in limb allometry between the two taxa emerges during ontogeny near an intermediate size threshold. Solnhofen avialans show increasingly positive PC2 values with growth, consistent with relatively greater forelimb elongation, as previously observed [16,32]. In contrast, *Anchiornis* shifts towards more negative PC2 scores as size increases, indicating relatively greater investment in hindlimb elongation. These patterns indicate that these two samples follow divergent allometric growth trajectories, respectively emphasizing either forelimb or hindlimb development, a distinction that possibly reflects differing functional or ecological strategies. Both the *Ostromia*/Haarlem specimen (near the middle) and *Alcmonavis* (the largest) fall tightly in the trend devised by specimens of *Archaeopteryx*.

(b) Validity of *Ostromia*

The Haarlem specimen (TM (Teylers Museum) 6928, 6929) is among the most poorly preserved and incomplete of the Urvogel specimens [1]. Three differences between the Haarlem specimen and other *Archaeopteryx* were identified [10]. A 'well-developed longitudinal furrow on the exposed medial side of the preserved manual phalanx I-1' [10] is a common taphonomic artefact observed in two-dimensionally crushed slab specimens of taxa with thin, hollow bones (figure 3; see electronic supplementary material). Most specimens of *Anchiornis*, like *Archaeopteryx*, are crushed, and these grooves, which are widely—but not

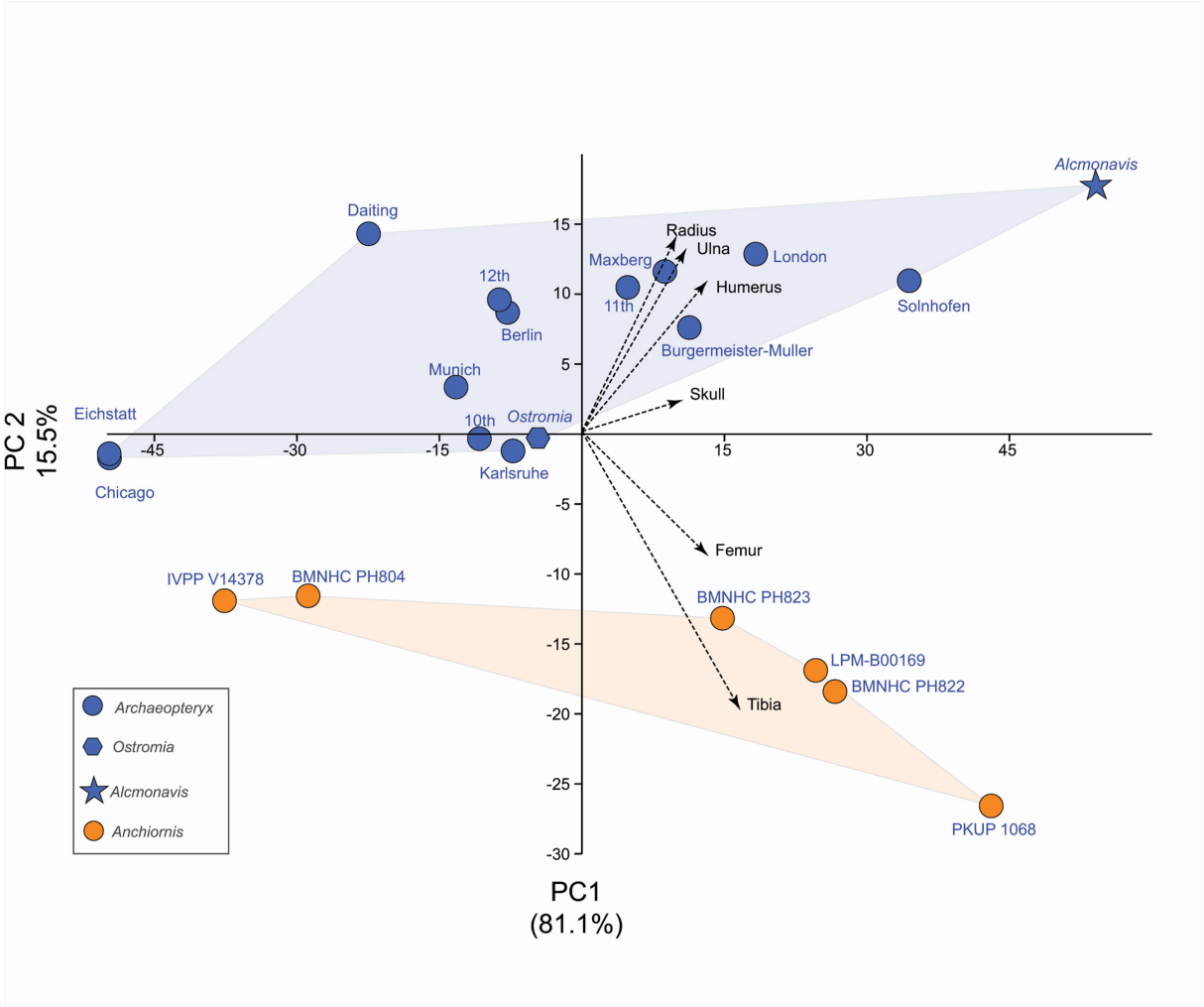

Figure 2. A principal component (PC) analysis scatterplot with dashed-black biplot vectors denoting measurement loadings on PCs. The direction of the vector indicates the loading value (positive or negative correlation) with PC scores and length of the vector indicates their magnitude of the correlation.

Table 3. Principal component (PC) analysis loadings. PCs 1 and 2 account for 96% of the total variation in the sample.

	PC1	PC2	PC3
skull	0.34247	0.072542	0.35068
humerus	0.42604	0.34737	0.16968
ulna	0.35475	0.42191	−0.1482
radius	0.32139	0.45021	−0.396
femur	0.42851	−0.28647	0.62803
tibia	0.53707	−0.64134	−0.52443

consistently—present, are not considered morphological features in recent descriptions [26,27]. Although this interpretation is acknowledged as a possibility [8], this feature was still used to differentiate this specimen from *Archaeopteryx* and align it with anchiornithines.

Two pubic features also purportedly distinguish the Haarlem specimen: the flexed pubic shaft and the shape of the pubic boot [10]. The flexed morphology appears to be the product of a break located close to the midpoint of the shaft (figure 3C). The boot is poorly preserved, overlapping the femora. Although described as having a nearly straight distal margin, it appears convex in published photographs [10, fig. 6a]. The caudodorsal margin of the boot is also described as lacking the cranial projection present in *Archaeopteryx* [10]. Although we tentatively observe an impression that we suggest is the cranial projecting portion of the caudodorsal margin of the boot (figure 3C), this interpretation, like any based on this specimen, is equivocal due to poor preservation, underscoring the tentative nature of any systematic acts based on this specimen.

Figure 3. Morphologies relevant to the taxonomy of the Solnhofen avialans. (A,B) Variable presence of taphonomic grooves in the manus of *Anchiornis* ((A) Shandong Tianyu Museum of Nature (STM) 0-143; (B) STM0-5)—note a groove extends the full length of the major and minor metacarpals in *Anchiornis* STM0-5 but not STM0-143, and a groove is present in the major digit phalanx 2 in STM0-5 but not STM0-143, consistent with the relatively poorer preservation of STM0-5; (C) photograph of the pubis of the Haarlem specimen TM 6928 (arrow indicates breakage producing the 'kink'; the dotted line represents interpretation of the mould of the missing portion of the pubic boot and the convex caudal margin) (photo by Luis Chiappe, used with permission); (D–F) Chicago *Archaeopteryx* Field Museum of Natural History (FMNH) PA 830 ((D) the right alular digit with taphonomic groove on distal half of the partially crushed phalanx I-1 indicated by arrow; (E) left proximal ulna with arrow indicating cotyla; (F) left distal ulna showing asymmetrical expansion). Scale bars equal 1 cm in (A–D); 0.5 mm in (E,F).

(c) Validity of *Alcmonavis*

The holotype of *Alcmonavis poeschli*, SNSB-BSPG (Staatliche naturwissenschaftliche Sammlungen Bayerns, Bayerische Staatssammlung für Paläontologie und Geologie) 2017 I 133, consists of a mostly crushed nearly complete forelimb [8]. It represents the largest avialan fossil recovered from the Solnhofen Limestones, >220% the size of the Chicago and Eichstätt specimens [8] (figure 2). Although its large size was previously considered at odds with the interpretation that it represents *Archaeopteryx* [8], the size range captured by the 15 Solnhofen avialan specimens is less than observed in *Anchiornis* and the basal pygostylian bird *Confuciusornis*. Using femoral length as a proxy for body size, the largest *Anchiornis* and *Confuciusornis* are 235.5 and 253% the size of the smallest, respectively [30,33,34], congruent with allometric observations (above). Given the size of SNSB-BSPG 2017 I 133, ontogeny should also be considered with regard to the expression of some features as purportedly diagnostic differences with *Archaeopteryx*.

SNSB-BSPG 2017 I 133 has a well-developed facet for the attachment of the m. pectoralis on the cranial margin of the deltopectoral crest that is considered absent in *Archaeopteryx* [8]. However, this region is preserved in only three specimens. As acknowledged, this region is damaged in the Thermopolis and London specimens, and the third (Maxberg specimen) is missing [8]. Therefore, the absence of this feature in *Archaeopteryx* should be considered equivocal. Although this margin is also poorly preserved in the Karlsruhe specimen, computed-tomographic data suggest this feature is absent [7]. Given the large size of SNSB-BSPG 2017 I 133, this scar may develop with advancing maturity.

Alcmonavis is diagnosed based on the unique combination of 10 characteristics [8], which we examine individually. A humerus with a 'large deltopectoral crest, with a maximal expansion that exceeds the width of the humeral shaft', is also present in specimens of *Archaeopteryx* [1,4]. Although the crest appears narrower in the Thermopolis specimen, the dorsal edge is also damaged and incomplete [15]. The proximal part of the humerus is described as strongly angled, forming an angle of approximately 38° with respect to the distal shaft. This is the most striking of the humeral morphologies, but given the very poorly preserved proximal half of the humerus (proximal fifth is missing), breakage (there are numerous cracks throughout the shaft) and slight disarticulation might explain this unusual angle, rendering this difference equivocal.

The ulna is described as having a 'well-defined, single, oval, concave proximal cotyla and small lateral tubercle' (labelled 'radial tubercle' [8, fig. 5A]); this feature is very slight and the bone margin is crushed such that this difference is ambiguous. In SNSB-BSPG 2017 I 133, the concave cotyla is on the cranial half of the proximal articular surface. The caudal half is poorly preserved. In the well-preserved Chicago *Archaeopteryx*, a similar cotyla located on the cranial half of the proximal articular surface of the ulna can be observed (figure 3E). The distal end of the ulna is described as 'slightly asymmetrically expanded', as in the Chicago *Archaeopteryx* (figure 3F). The presence of a 'large, crest-like biceps tubercle on the proximal radius' cannot be validated due to the very poor preservation of the proximal radius in SNSB-BSPG 2017 I 133. While the biceps tubercle is clearly present in this specimen and also documented in *Archaeopteryx* [8], whether this structure was crest-like is ambiguous; the radius is crushed such that the distal end of this tubercle could be a preservational artefact and the length of the crest connecting the proximal biceps tubercle with the elevated distal fragment is mostly reconstructed [8]. The 'longitudinal groove along the medial side of the radial shaft' and on phalanx I-1 are both taphonomic artefacts of crushed two-dimensional preservation (see electronic supplementary material). Although not described, similar grooves are also present on metacarpals II and III in SNSB-BSPG 2017 I 133 [8]. Metacarpal II is described as 'considerably more robust than metacarpal I and III', a condition also present in the Solnhofen *Archaeopteryx*, which is closest in size to SNSB-BSPG 2017 I 133 [1]. This may indicate that metacarpal II becomes more robust during ontogeny. Proportional differences may also be exaggerated by the fact the metacarpals are exposed in caudal view in SNSB-BSPG 2017 I 133, instead of the more typical exposure in ventral or dorsal view. Phalanx II-1 is described as 'very robust, but with rounded, rather than flattened cross-section'; however, crushing prevents assessment of cross-sectional shape. Similarly, whether phalanx II-1 is 'slightly twisted' is difficult to validate in a flattened structure. Lastly, the large Solnhofen specimen, the second largest Solnhofen avialan after *Alcmonavis*, also preserves 'manual unguals with strongly developed and palmarly transversely expanded flexor tubercles', suggesting these tubercles enlarge with maturity in *Archaeopteryx*.

5. Discussion

Morphometric analysis of all 15 known avialan fossils from the Solnhofen Limestone indicates that proportionately, these specimens fit consistently in a growth curve (figure 1). This indicates that skeletal proportions align with the interpretation that all specimens represent a single taxon, *Archaeopteryx*, as has been previously suggested based on a smaller sample [16,17]. This is not unexpected given recent analyses that suggest these fossils only span 700 000–1 000 000 years [7]. If more than one taxon is present as has been suggested [8,10], they share the same limb-scaling pattern for a given size, which does not support the hypothesis that non-avian anchiornithine avialans, archaeopterygid avians and non-archaeopterygid avians are all represented by this sample.

To test the hypothesis that *Anchiornis* is capable of volant locomotion [35] and the interpretation that *Ostromia* (Haarlem specimen) is a non-avian avialan closely related to anchiornithines [10], we included *Anchiornis* in our dataset [25–27]. *Anchiornis* specimens cluster distinctly and separately from all Solnhofen avialans, including the Haarlem specimen which clusters with other *Archaeopteryx*, indicating that morphometrics do not support the hypothesis that *Ostromia* represents a distinct taxon and a non-avian anchiornithine avialan. Compared to *Anchiornis*, specimens of *Archaeopteryx* (Haarlem included) show a distinct pattern in which larger individuals have proportionately longer forelimbs [16,32] (figure 2). The same pattern is observed in the Mesozoic birds *Confuciusornis* [36] and *Archaeorhynchus* [37] and is consistent with scaling trends in the wings of neornithines [38]. *Anchiornis* shows the opposite pattern in which larger specimens have proportionately longer hindlimbs. This likely reflects ecological differences between these taxa and strongly suggests that *Anchiornis* was non-volant, as also suggested by wing structure [26,39] and moult strategy [40]. These differences in proportions begin at intermediate growth stages, indicating these two taxa share similar growth patterns, consistent with interpretations they are closely related [3]. Compared to *Archaeopteryx*, sampled *Anchiornis* specimens show much greater proportional variation, not falling along a tight regression like *Archaeopteryx* (figure 1) and also observed in *Confuciusornis* [41]. We suggest this is also the result of locomotor differences, in which the proportions of the volant *Archaeopteryx* (and *Confuciusornis*) are more constrained by the biomechanics of aerodynamic locomotion. The dispersion of the sample does not suggest these proportional differences represent unrecognized taxonomic diversity.

Rauhut *et al.* provided a revised diagnosis for the genus *Archaeopteryx* [9], which allows the London, Berlin, Eichstätt, Solnhofen, Daiting, Thermopolis, 11th, 12th and Chicago specimens to be assigned to this genus [4,9]. The Karlsruhe specimen

is additionally assigned to *Archaeopteryx* based on the similar morphology of preserved elements [7]. Rauhut *et al.* suggest the missing Maxberg specimen is probably referrable to this genus and the incomplete Bürgermeister-Müller specimen might be referable, although certainty is precluded by the loss of the Maxberg specimen and the fragmentary preservation of the Bürgermeister-Müller specimen [9]. The Haarlem specimen and SNSB-BSPG 2017 I 133, interpreted as distinct genera, are also characterized by incomplete and poor preservation. We examined the justification that each of these specimens is not *Archaeopteryx* and found the evidence to be tentative at best. Considering the poor quality of these specimens, interpretations regarding their uniqueness should be considered carefully and, like identifications concerning the very incomplete Bürgermeister-Müller specimen, conclusions should be tentative. Examination of the characteristics used to diagnose 'Alcmonavis' reveals that while some are most likely taphonomic artefacts (e.g. angled proximal end of humerus, groove on the radius), some may be ontogenetic (proportions of the metacarpals and manual flexor tubercles, muscle scar on humerus) and some cannot be verified given that the specimen is mostly crushed (e.g. cross-section and twisting of the first phalanx of the major digit). Still others do not appear to clearly distinguish SNSB-BSPG 2017 I 133 from *Archaeopteryx* (e.g. size of the deltopectoral crest). The morphometric data presented here further weaken interpretations that these specimens represent different taxa, supporting the interpretation that observed differences with 'Alcmonavis' may be ontogenetic. Similarly, purported differences with regard to 'Ostromia' and *Archaeopteryx* are either taphonomic (longitudinal groove on manual phalanx I-1, flexed pubis) or cannot be confirmed due to unclear preservation (shape of the pubic boot).

6. Conclusion

Morphometric analysis of all 15 known Solnnhofen avialans and five published specimens of *Anchiornis* provides critical insights regarding the taxonomy of *Archaeopteryx* and transformations across the dinosaur–bird transition. The absence of outliers in the morphometrics dataset of Solnhofen avialans suggests that the most parsimonious interpretation of the sample is that all 15 specimens represent a single taxon along a growth curve. Our approach highlights the value of integrating allometric constraints into imputations for fragmentary fossils, allowing incomplete specimens to be contextualized without introducing analytical bias. Changes in proportions associated with size support the interpretation that *Archaeopteryx* was volant. Differences in variation, proportions and proportional changes with size between *Archaeopteryx* and *Anchiornis* support interpretations that the latter was non-volant. Morphological arguments regarding the taxonomy of TM 6928/6929 and SNSB-BSPG 2017 I 133 are obfuscated by poor preservation such that interpretations that these specimens represent distinct genera are equivocal.

Ethics. This work did not require ethical approval from a human subject or animal welfare committee.

Data accessibility. All data used for the analyses presented can be found in tables 1 and 2 (and comes from previously published sources). Analyses were run using the computer program SPSS [26].

Supplementary material is available online [42].

Declaration of AI use. We have not used AI-assisted technologies in creating this article.

Authors' contributions. J.O.: investigation, visualization, writing—original draft, writing—review and editing; J.M.-L.: conceptualization, formal analysis, visualization, writing—original draft, writing—review and editing.

Both authors gave final approval for publication and agreed to be held accountable for the work performed therein.

Conflict of interest declaration. We declare we have no competing interests.

Funding. No funding has been received for this article.

References

1. Wellnhofer P. 2009 *Archaeopteryx: the icon of evolution*. Munich, Germany: Verlag Dr. Friedrich Pfeil.
2. von Meyer H. 1861 *Archaeopteryx litographica* (Vogel-Feder) und *Pterodactylus* von Solenhofen. *Neues Jahrb. Mineral. Geogn. Geol. Petrefakt.-Kde.* **1861**, 678–679.
3. Chen R *et al*. 2025 Earliest short-tailed bird from the Late Jurassic of China. *Nature* **638**, 441–448. (doi:10.1038/s41586-024-08410-z)
4. O'Connor J *et al*. 2025 Chicago *Archaeopteryx* informs on the early evolution of the avian bauplan. *Nature* **641**, 1201–1207. (doi:10.1038/s41586-025-08912-4)
5. Foth C, Tischlinger H, Rauhut OWM. 2014 New specimen of *Archaeopteryx* provides insights into the evolution of pennaceous feathers. *Nature* **511**, 79–82. (doi:10.1038/nature13467)
6. Mayr G, Pohl B, Peters DS. 2005 A well-preserved *Archaeopteryx* specimen with theropod features. *Science* **310**, 1483–1486. (doi:10.1126/science.1120331)
7. Foth C *et al*. 2025 A new *Archaeopteryx* from the lower Tithonian Mörnsheim Formation at Mühlheim (Late Jurassic). *Foss. Rec.* **28**, 17–43. (doi:10.3897/fr.28.e131671)
8. Rauhut OWM, Tischlinger H, Foth C. 2019 A non-archaeopterygid avialan theropod from the Late Jurassic of southern Germany. *eLife* **8**, 1–38. (doi:10.7554/eLife.43789)
9. Rauhut OWM, Foth C, Tischlinger H. 2018 The oldest *Archaeopteryx* (Theropoda: Avialiae): a new specimen from the Kimmeridgian/Tithonian boundary of Schamhaupten, Bavaria. *PeerJ* **6**, e4191. (doi:10.7717/peerj.4191)
10. Foth C, Rauhut OWM. 2017 Re-evaluation of the Haarlem *Archaeopteryx* and the radiation of maniraptoran theropod dinosaurs. *BMC Evol. Biol.* **17**, 1–16. (doi:10.1186/s12862-017-1076-yx)
11. Ostrom JH. 1970 *Archaeopteryx*: notice of a 'new' specimen. *Science* **170**, 537–538. (doi:10.1126/science.170.3957.537)
12. Von Meyer H. 1857 Beiträge zur näheren Kenntnis fossiler Reptilien. *Neues Jahrb. Mineral. Geogn. Geol. Petrefakt.-Kde.* 532–543.
13. Kundrát M, Nudds J, Kear BP, Lü JC, Ahlberg PE. 2019 The first specimen of *Archaeopteryx* from the Upper Jurassic Mörnsheim Formation of Germany. *Hist. Biol.* **31**, 3–63. (doi:10.1080/08912963.2018.1518443)
14. Wellnhofer P. 1993 Das siebte exemplar von *Archaeopteryx* aus den Solnhofer Schichten. *Archaeopteryx* **11**, 1–47.
15. Mayr G, Pohl B, Hartman S, Peters DS. 2007 The tenth skeletal specimen of *Archaeopteryx*. *Zool. J. Linn. Soc.* **149**, 97–116. (doi:10.1111/j.1096-3642.2006.00245.x)
16. Senter P, Robins JH. 2003 Taxonomic status of the specimens of *Archaeopteryx*. *J. Vertebr. Paleontol* **23**, 961–965. (doi:10.1671/22)

17. Houck MA, Gauthier JA, Strauss RE. 1990 Allometric scaling in the earliest *Archaeopteryx lithographica*. *Science* **247**, 195–198. (doi:10.1126/science.247.4939.195)
18. Gauthier J. 1986 Saurischian monophyly and the origin of birds. In *The origin of birds and the evolution of flight* (ed. K Padian), pp. 1–55. San Francisco, CA: California Academy of Sciences.
19. Field DJ, Benito J, Chen A, Jagt JWM, Ksepka DT. 2020 Late Cretaceous neornithine from Europe illuminates the origins of crown birds. *Nature* **579**, 397–401. (doi:10.1038/s41586-020-2096-0)
20. Godefroit P, Cau A, Dong-Yu H, Escuillié F, Wenhao W, Dyke G. 2013 A Jurassic avialan dinosaur from China resolves the early phylogenetic history of birds. *Nature* **498**, 359–362. (doi:10.1038/nature12168)
21. Xu L *et al*. 2023 A new avialan theropod from an emerging Jurassic terrestrial fauna. *Nature* **621**, 336–343. (doi:10.1038/s41586-023-06513-7)
22. Haeckel E. 1866 *Generelle morphologie der organismen*. Berlin, Germany: Verlag von Georg Reimer.
23. Gianechini FA, Makovicky PJ, Apesteguía S, Cerda IA. 2018 Postcranial skeletal anatomy of the holotype and referred specimens of *Buitreraptor gonzalezorum* Makovicky, Apesteguía and Agnolín 2005 (Theropoda, Dromaeosauridae), from the Late Cretaceous of Patagonia. *PeerJ* **6**, e4558. (doi:10.7717/peerj.4558)
24. Sereno PC. 1997 The origin and evolution of dinosaurs. *Annu. Rev. Earth Planet. Sci.* **25**, 435–489. (doi:10.1146/annurev.earth.25.1.435)
25. Xu X, Zhao Q, Norell MA, Sullivan C, Hone DW, Erickson GM, Wang XL, Han FL, Guo Y. 2009 A new feathered maniraptoran dinosaur fossil that fills a morphological gap in avian origin. *Chin. Sci. Bull.* **54**, 430–435. (doi:10.1007/s11434-009-0009-6)
26. Hu D, Hou L, Zhang L, Xu X. 2009 A pre-*Archaeopteryx* troodontid theropod from China with long feathers on the metatarsus. *Nature* **461**, 640–643. (doi:10.1038/nature08322)
27. Pei R, Li QG, Meng QJ, Norell MA, Gao KQ. 2017 New specimens of *Anchiornis huxleyi* (Theropoda: Paraves) from the Late Jurassic of Northeastern China. *Bull. Am. Mus. Nat. Hist.* **411**, 1–67. (doi:10.1206/0003-0090-411.1.1)
28. Baraldi AN, Enders CK. 2010 An introduction to modern missing data analyses. *J. Sch. Psychol.* **48**, 5–37. (doi:10.1016/j.jsp.2009.10.001)
29. Ilin A, Raiko T. 2010 Practical approaches to principal component analysis in the presence of missing values. *J. Mach. Learn. Res.* **11**, 1957–2000.
30. Marugán-Lobón J, Chiappe LM. 2022 Ontogenetic niche shifts in the Mesozoic bird *Confuciusornis sanctus*. *Curr. Biol.* **32**, 1629–1634. (doi:10.1016/j.cub.2022.02.010)
31. IBM. 2023 SPSS statistics for windows (version 28.0). See https://www.ibm.com/docs/en/spss-statistics.
32. Wellnhofer P. 1974 Das funfte skelettexemplar von *Archaeopteryx*. *Palaeontogr. Abt. A* **147**, 169–215.
33. Zhou YB, Pan YH, Wang M, Wang XL, Zheng XT, Zhou ZH. 2024 Fossil evidence sheds light on sexual selection during the early evolution of birds. *Proc. Natl Acad. Sci. USA* **121**, 1–9. (doi:10.1073/pnas.2309825120)
34. Zheng XT, O'Connor JK, Wang XL, Wang M, Zhang XM, Zhou ZH. 2014 On the absence of sternal elements in *Anchiornis* (Paraves) and *Sapeornis* (Aves) and the complex early evolution of the avian sternum. *Proc. Natl Acad. Sci. USA* **111**, 13900–13905. (doi:10.1073/pnas.141107011)
35. Pei R *et al*. 2020 Potential for powered flight neared by most close avialan relatives, but few crossed its thresholds. *Curr. Biol.* **30**, 4033–4046. (doi:10.1016/j.cub.2020.06.105)
36. Marugán-Lobón J, Chiappe LM, Ji S, Zhou Z, Chunling G, Hu D, Meng Q. 2011 Quantitative patterns of morphological variation in the appendicular skeleton of the Early Cretaceous bird *Confuciusornis*. *J. Syst. Palaeontol.* **9**, 91–101. (doi:10.1080/14772019.2010.517786)
37. Foth C, Wang SY, Spindler F, Lin Y, Yang R. 2021 A juvenile specimen of *Archaeorhynchus* sheds new light on the ontogeny of basal euornithines. *Front. Earth Sci.* **9**, 1–19. (doi:10.3389/feart.2021.604520)
38. Sullivan TN, Meyers MA, Arzt E. 2019 Scaling of bird wings and feathers for efficient flight. *Sci. Adv.* **5**, eaat4269. (doi:10.1126/sciadv.aat4269)
39. Kiat Y, O'Connor JK. 2024 Functional constraints on the number and shape of flight feathers. *Proc. Natl Acad. Sci. USA* **121**, 1–11. (doi:10.1073/pnas.2306639121)
40. Kiat Y, Wang X, Zheng X, Wang Y, O'Connor J. 2025 Wing morphology of *Anchiornis huxleyi* and the evolution of molt strategies in paravian dinosaurs. *Commun. Biol.* **8**, 1633. (doi:10.1038/s42003-025-09019-2)
41. Chiappe LM, Marugán-Lobón J, Ji S, Zhou Z. 2008 Life history of a basal bird: morphometrics of the Early Cretaceous *Confuciusornis*. *Biol. Lett.* **4**, 719–723. (doi:10.1098/rsbl.2008.0409)
42. O'Connor J, Marugán-Lobón J. 2026 Supplementary material from: Evaluating variation in Solnhofen avialans. Figshare. (doi:10.6084/m9.figshare.c.8342754)